Environmental Science and Ecotechnology 10 (2022) 100163

Contents lists available at ScienceDirect

Environmental Science and Ecotechnology

journal homepage: www.journals.elsevier.com/environmental-science-and-ecotechnology/

Original Research

Overlying water fluoride concentrations influence dissolved organic matter composition and migration from pore water in sediment via bacterial mechanisms

Xiang Zhu [a, 1], Zibo Wang [b, 1], Yidan Luo [a, c], Yushen Ma [a, c], Zhipeng Xu [a, c], Longmian Wang [a, *], Fuquan Peng [a], Qingqing Pang [a], Yiping Li [c], Fei He [a, **], Bin Xu [a]

[a] Nanjing Institute of Environmental Sciences, Ministry of Ecology and Environment, Nanjing, 210042, PR China
[b] China National Environmental Monitoring Centre, No8-2 Anwai Dayangfang, Chaoyang District, Beijing, 100012, PR China
[c] College of Environment, Hohai University, Nanjing, 210098, PR China

ARTICLE INFO

Article history:
Received 11 September 2021
Received in revised form
23 February 2022
Accepted 23 February 2022

Keywords:
Fluoride fluctuation
Dissolved organic matter
Fluorescent components
Bacterial abundances
Enzyme variation

ABSTRACT

Fluoride (F^-) is widespread in aquatic environments; however, it is not clear whether the fluctuation of F^- concentrations in overlying lake water affects the composition and migration of dissolved organic matter (DOM) from sediment. A case study was presented in Sand Lake, China, and an experiment was conducted to analyze the influence of different F^- concentrations in overlying water on DOM characteristics. Diffusion resulted in similarities in DOM components between overlying and pore waters, and bacterial activities and enzyme variation resulted in differences between them. Higher F^- concentrations in overlying water resulted in a higher pH of pore water, which favored the enrichment of protein-like substances. Higher F^- concentrations caused lower DOM concentrations and lower maximum fluorescence intensities (F_{max}) of protein-like components in pore water. The F^- concentrations had significantly negative correlations with Shannon indexes ($P < 0.05$). *Thiobacillus* influenced the migration of tyrosine-like substances by decreasing the pH of pore water. *Trichococcus* and *Fusibacter* altered the F_{max} of protein-like, humic-like, and fulvic-like substances. The F^- concentrations affected the DOM composition and migration due to the response of functional bacterial communities, which were positively correlated with the relative abundance of *Thiobacillus* and negatively correlated with the relative abundances of *Trichococcus* and *Fusibacter*. The high F^- concentrations influenced the biosynthesis and degradation of protein-like substances by shifting the abundances of the relevant enzymes. The results of this study may provide ideas for investigating DOM cycling under the influence of F^-, especially in lakes with fluctuations in F^- concentrations.

1. Introduction

Dissolved organic matter (DOM) plays a vital role in aquatic ecosystems, and its content and composition influence biogeochemical processes, including bacterial activities, nutrient cycling and pollutant transport [1,2]. Sediments act as an important source of DOM in the water column, especially in shallow lakes [3]. Hydrolysis and depolymerization of particulate organic matter (POM) and lysis of benthic bacterial cells in sediments are the main reasons for DOM release into pore water, which leads to orders of magnitude higher concentrations of DOM in pore water than in overlying water [4,5]. The transport of DOM from pore water to overlying water is mainly driven by diffusion [6], which together with biogeochemical processes results in differences in DOM composition and fluorescence characteristics between pore water and the overlying water column.

Compared to DOM in overlying water, DOM in pore water usually has higher molecular formula richness and more humic-like fluorescent components [4]. A large amount of the DOM released from the sediments can be mineralized at the sediment-water interface [7]. Many environmental and biological factors affect

* Corresponding author.
** Corresponding author.
E-mail addresses: wlmian@sina.com (L. Wang), hefei@nies.org (F. He).
[1] Co-first authorship.

https://doi.org/10.1016/j.ese.2022.100163

DOM transformation processes. pH is an important factor controlling DOM solubility, and increasing alkalinity is well known to cause DOM desorption with increasing charge density for DOM [8,9]. Redox conditions and bacterial degradation also cause changes in DOM composition and release rate [1,10].

Bacteria can modulate the quantity and quality of DOM in sediment and ultimately influence carbon cycling in lake systems [11]; the mechanisms mainly include biodegradation, desorption stimulation, and metabolism [5,12,13]. It was reported that bacterial compositions and abundances are associated with DOM composition [14]. The alpha diversity of bacteria was strongly correlated with the bulk concentrations and molecular numbers of DOM [15]. Benthic bacterial communities produce fresh DOM compounds via the usage of organic matter in sediment as energy and carbon sources [16], and different bacterial species affect the specific DOM components. *Trichococcus* is considered to participate in protein decomposition [17]. *Cloacimonetes* and *Marinimicrobia* have versatile roles in DOM degradation [18]. F^- is widespread in aquatic environments and causes approximately 200 million people to suffer from dental and skeletal fluorosis [19]. F^- has been demonstrated to be toxic to bacteria [20] and affects biocenosis in soil and groundwater [21,22]. The toxicity of F^- is broadly mediated via four mechanisms: protein inhibition, organelle disruption, pH alteration, and electrolyte imbalance [23]. Therefore, the main hypothesis of this study was that the F^- concentrations influence bacterial communities and the relevant enzymes in sediment and then cause the variation in DOM composition in both overlying water and pore water.

High levels of F^- in lake ecosystems are common in semiarid areas [24], and the F^- enrichment environment and artificial management probably resulted in fluctuations in F^- concentrations [25]. However, whether the fluctuations of F^- concentrations influence the DOM cycling in the lake system has not been determined. Herein, a case study was presented in Sand Lake, a typical lake in a semiarid area whose F^- concentrations have fluctuated from 0.78 mg L^{-1} to 1.59 mg L^{-1} in recent years [26]. This study makes one of the first attempts to ascertain (1) the variation in pH and fluorescence characteristics of DOM in both overlying water and pore water under different F^- concentrations; (2) the response of bacterial communities and enzymes related to DOM transformation in sediment to F^- stress in lake water; and (3) the interaction among the DOM fluorescence characteristics, F^- concentrations, pH and bacterial community characteristics in pore water. The results of this study may provide ideas for investigating DOM migration and cycling under F^- stress, especially in lakes with fluctuations in F^- concentrations.

2. Materials and methods

2.1. Site description

Sand Lake (106°18′ E, 38°45′ N) is a famous tourist attraction in Shizuishan city, Ningxia Hui Autonomous Region, China (Fig. 1). Sand Lake has a surface area of 13.96 km^2 and a mean depth of 2.2 m [27]. The climate of this region is characterized by arid or semiarid conditions with intense evaporation. Sand Lake is located in an area suitable for F^- enrichment, the total F^- concentrations of the soil around the lake were reported to range from 443 to 2790 mg kg^{-1}, and the total F^- concentrations of the lake sediment were reported to range from 936 to 1682 mg L^{-1} [25].

2.2. Sample collection and analysis

Sediment and lake water samples were collected in November 2020. As shown in Fig. 1, the sampling site (106°21′19.6″ E,38°49′2.3″ N) is far from the tourist area and possible pollution sources (including the hotel, sand dune, and bird habitats). Before water sampling, the sampling bottles were rinsed 2–3 times with deionized water and lake water. The water samples were collected at a depth of 30 cm below the water surface, transferred to the laboratory within 24 h, and stored at 4 °C for further analysis within 48 h. Surface sediment samples were collected by a gravity collector and stored at −80 °C via dry ice during sampling and transport. The sediment was used for the experiment immediately after arriving at the laboratory. The physical and chemical parameters of lake water and sediment were analyzed in triplicate, the mean values of which are shown in Table 1 and Table 2, respectively. The analytical methods and their corresponding resources, equipment, and detection limits are listed in Table A1 and Table A2.

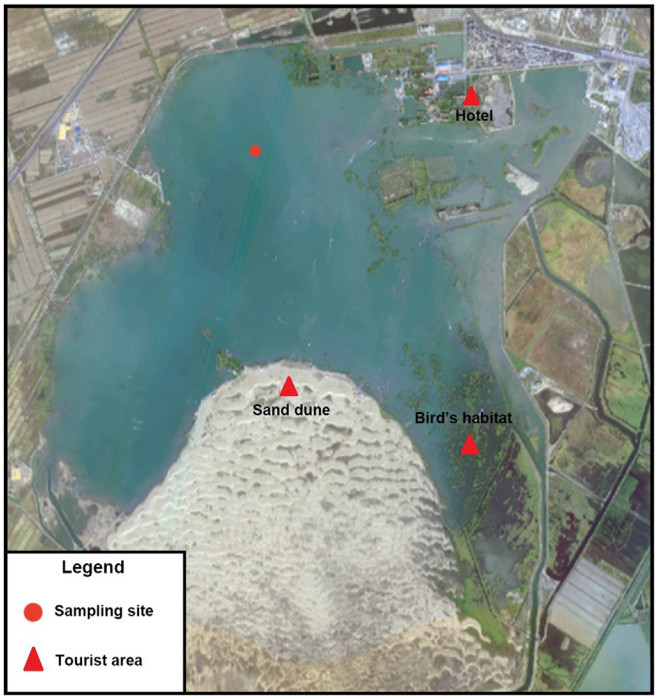

Fig. 1. Location of Sand Lake and sampling sites.

2.3. Experimental processes

The experiment was conducted in polyvinyl chloride (PVC) cylinders in the dark. The diameter and height of each cylinder were 9 cm and 60 cm, respectively. Before the experiment, 20 cm of sediment was laid at the bottom of the cylinders. The simulated lake water was prepared as the overlying water based on the analysis of lake water (Table 1), the depth was 30 cm, and the preparation method is shown in Table A5.

Four experimental groups were set up, whose F^- concentrations in the overlying water were 0.5 times (0.345 mg L^{-1}, designated as 0.5F), 1 time (0.69 mg L^{-1}, designated as 1F), 2 times (1.38 mg L^{-1}, designated as 2F), and 4 times (2.76 mg L^{-1}, designated as 4F) that of the raw water. The F^- concentrations were regulated by sodium fluoride. A sterilized group was set up, the F^- concentration in the overlying water of which was 0.69 mg L^{-1} (sign as 1F#). The sediment in the sterilized group was irradiated with ^{60}Co γ-rays at a dose of 30000 Gy at 0 °C. Before the experiment, the sediments were incubated in the dark for 3 days. The overlying water and pore water subsamples were collected at 0 d, 1 d, 2 d, 3 d, 5 d, 7 d, 10 d, 15 d, 20 d, and 30 d. The overlying water (5 ml each time) was

Table 1
The physical and chemical characteristics of lake water.

Number	Parameters	Concentrations	Number	Parameters	Concentrations
1	pH	8.83	8	Cl^-	256.6
2	COD	26	9	SO_4^{2-}	272.4
3	TP	0.02	10	HCO_3^-	96.1
4	TN	0.9	11	Na^+	155.0
5	NO_3^--N	0.33	12	K^+	8.1
6	NH_4^+-N	0.17	13	Ca^{2+}	41.9
7	F^-	0.69	14	Mg^{2+}	68.1

Units: dimensionless for pH, and mg L^{-1} for others.

Table 2
The physical and chemical characteristics of sediment.

Parameters	Organic Matter	Moisture content	TN	TP	Total F^-	Water-souble F^-
Concentrations	3.1	69.4	2751.5	549.9	1417.0	8.3

Units: % for organic matter and moisture content, and mg kg^{-1} for others.

sampled at a depth of 10 cm below the water surface, and the pore water (5 ml each time) was sampled at a depth of 5 cm below the sediment-water interface. The overlying water and pore water subsamples were collected by a syringe and Rhizon sampler (FLEX, Rhizosphere, Netherlands), respectively, and filtered through a 0.45 μm cellulose membrane filter. The simulated raw water was slowly replenished along the column wall after sampling. Before and after the experiment, sediment subsamples were collected for high-throughput sequencing analysis.

2.4. DOM spectroscopic measurements and parallel factor analysis (PARAFAC)

The samples of overlying water and pore water (three analytical replicates) were measured, the numbers of which were both 150. The pore water samples were diluted 5 times before measurement. Absorption spectra were scanned from 200 to 800 nm at 1 nm intervals by an ultraviolet visible spectrometer (UV-2550, Shimadzu, Japan). Fluorescence excitation-emission matrices (EEMs) were obtained by a fluorescence spectrophotometer (F-7000, Hitachi, Japan). The excitation wavelengths ranged from 200 nm to 450 nm in 5 nm intervals, and the emission wavelengths ranged from 250 nm to 600 nm in 1 nm intervals. PARAFAC was conducted in MATLAB (MathWorks, USA). The primary and secondary Rayleigh scattering regions were eliminated, and the inner-filter effects were corrected.

Several parameters were calculated by ultraviolet absorption spectra and corrected EEMs. The absorption coefficient represents the abundance of dissolved organic carbon, and the formula is as follows [28,29]:

$$a(355) = 2.303(OD)/r \quad (1)$$

a(355) is the absorption coefficient at a wavelength of 355 nm, *OD* is the optical density at a wavelength of 355 nm, and *r* is the path length (m).

The humification index (HIX) represented the degree of DOM humification, which was calculated by the ratio of the emission spectra integral value between 435–480 nm and 300–345 nm when excitation equals 254 nm [30]. The biological index (BIX) represented the autochthonous contribution of DOM, which was calculated by the ratio of the emission fluorescence intensity of 380 nm–430 nm when excitation equals 310 nm [31]. The maximum fluorescence intensities (F_{max}) were used to estimate the relative abundances of components identified from PARAFAC.

2.5. High-throughput sequencing analysis

The original sediment and the sediment subsamples of each group after the experiment were measured by high-throughput sequencing analysis in duplicate, and the total number of samples was 11. Total genomic DNA samples were extracted by an Omega Soil DNA Kit (D5625–01, Omega bio TEK, USA) from 0.25 g sediment samples, and DNA quantity and quality were detected by spectrophotometry (NanoDropND-1000, ThermoFisher, USA) and 1.2% agarose gel electrophoresis, respectively. The V3–V4 regions of 16S rRNA were amplified by PCR using forward primer 338F (5'-ACTCCTACGGGAGAGGCAGCA-3') and reverse primer 806R (5'-GGACTACHVGGGTWTCTAAT-3'). The PCR amplification conditions were as follows: predenaturation for 5 min at 98 °C, 25 cycles of denaturation for 30 s at 98 °C, annealing for 30 s at 53 °C, extension for 45 s at 72 °C, and final extension for 5 min at 72 °C. The PCR amplicons were purified by Vazyme VAHTSTM DNA Clean Beads (Vazyme, China) and quantified by a Quant-iT PicoGreen dsDNA Assay Kit (Invitrogen, USA). Sequencing was performed using the Illumina MiSeq platform and MiSeq Reagent Kit v3 by Personal Biotechnology Co., Ltd. (Shanghai, China). The sequences generated in this study were deposited in the National Centre for Biotechnology Information under accession number SRP321026.

2.6. Data analysis and plotting

Data analyses were conducted using Microsoft Excel 2019. One-way analysis of variance (ANOVA) was conducted using R 3.6.3 [32]. Pearson's correlation analysis and redundancy analysis were performed and plotted by R 3.6.3. Other graphs were constructed using Origin 2017.

3. Results

3.1. pH variation of overlying water and pore water

The pH variation of overlying water and pore water is shown in Fig. 2. The pH decreased with time in both overlying water and pore water. The pH of the overlying water ranged from 6.7 to 7.0 after the experiment, and their values in the 0.5F group were lower than those in the other groups. The pH of pore water ranged from 6.7 to 7.5, and their values in the 0.5F group were significantly lower than those in the other groups except for 1F# ($P < 0.05$).

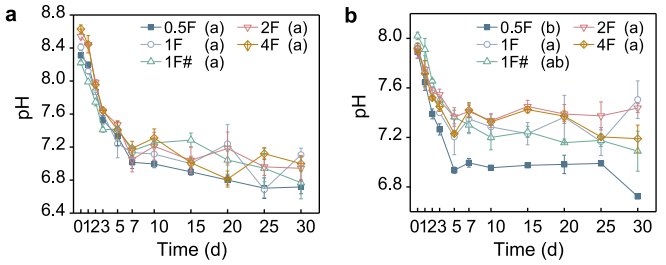

Fig. 2. pH of overlying water (**a**) and pore water (**b**). Different letters in brackets indicate significant differences at $P < 0.05$ according to Tukey's test.

3.2. Fluorescence characteristics of DOM

As shown in Fig. 3a and d, the a(355) of overlying water and pore water both increased over time in each group. The a(355) values of 2F and 4F were obviously lower than those of the other groups in overlying water and pore water, which represented lower DOM concentrations. The HIX of overlying water was higher than that of pore water, and its values in the sterilized group were higher than those of the other groups. The BIX values in overlying water were higher than those in pore water. There were no significant differences in BIX among the groups in either overlying water or pore water ($P > 0.05$).

3.3. PARAFAC of DOM

Four different fluorescent components were identified from the overlying water (Fig. 4), named C1, C2, C3, and C4. The four different fluorescent components affirmed in pore water were named C1p, C2p, C3p, and C4p. (Fig. 5). The results of PARAFAC were based on the split-half validation procedure and analysis of residuals. The fluorescence characteristics of the four components are shown in Table A3, and the temporal variation in F_{max} is shown in Fig. A1 and Fig. A2. In overlying water, the F_{max} values of C1, C3 and C4 in the sterilized group were significantly higher than those in the other groups ($P < 0.05$), and there were no significant differences between the groups without sterilization. It is worth noting that the mean F_{max} of C4 in group 4F was higher than that in the other groups without sterilization, especially after 7 days (Fig. A1). The proportions of C2 and C3 in group 4F were closer to those in the sterilized group. In pore water, the F_{max} of C1p in group 2F was the lowest, which was significantly lower than that in the sterilized group ($P < 0.05$) and had no significant differences from those in the other groups. The F_{max} of C2p in group 2F was the lowest, which was significantly lower than that in group 0.5F ($P < 0.05$) and was not significantly different from those in the other groups. The F_{max} of C4p in the sterilized group was the highest, with the values in group 4F being higher than those in other groups without sterilization over the course of the experiment. There were no significant differences in the proportions of identical components among the groups without sterilization. As shown in Fig. A2, the F_{max} of C1p and C3p in each group tended to decrease over time. The decline in the F_{max} of C1p in group 4F was higher than that in the other groups, and the decline in the F_{max} of C2p and C3p in groups 0.5F and 4F was higher than that in the other groups. The F_{max} values of DOM components in groups 1F and 4F were significantly different in the early stage of the experiment (Fig A1 and A2) and became similar in the late stages of the experiment.

3.4. 16S rRNA gene sequencing of sediment bacteria

The alpha diversity indexes of sediment bacteria are presented in Table A4, where "Original" means the original sediments before the experiment. The Chao1 index represents bacterial species

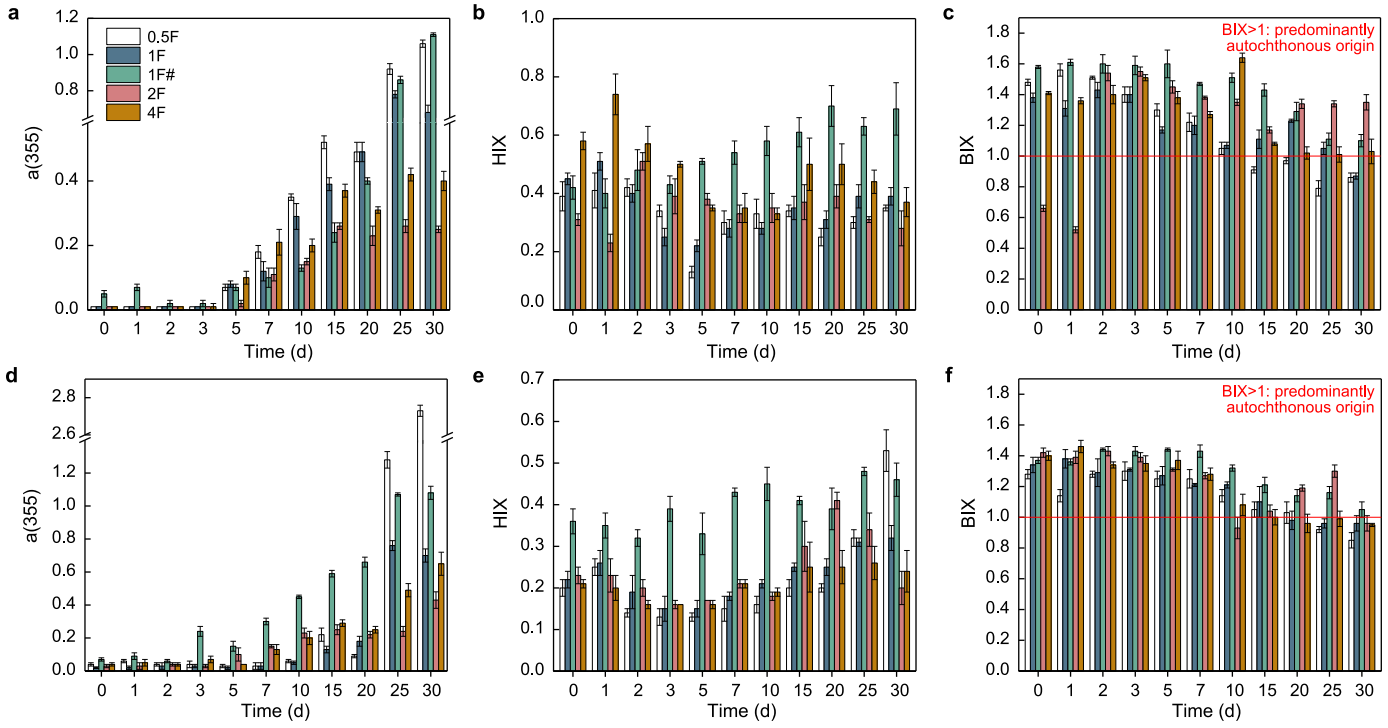

Fig. 3. Fluorescence characteristics of DOM: **a**, a(355) of overlying water; **b**, HIX of overlying water; **c**, BIX of overlying water; **d**, a(355) of pore water; **e**, HIX of pore water; **f**, BIX of pore water.

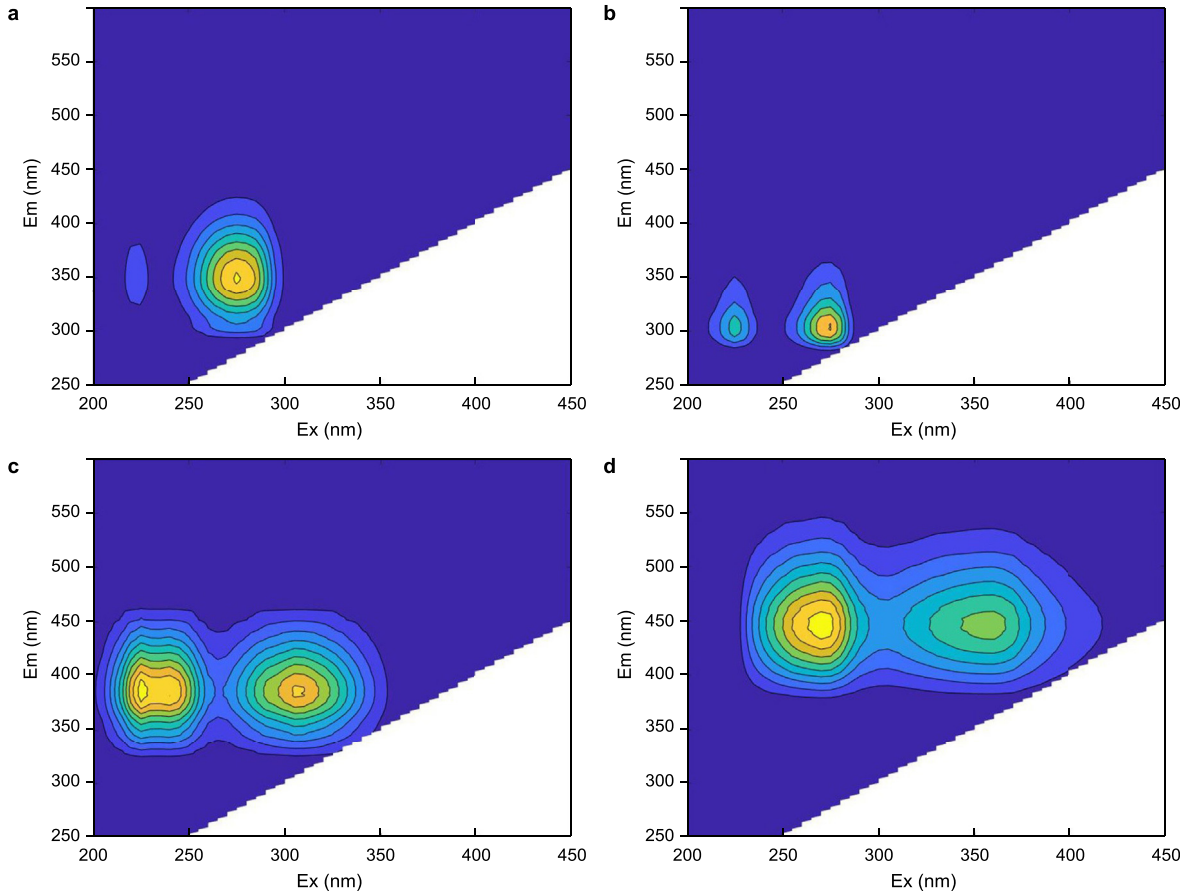

Fig. 4. PARAFAC of DOM in overlying water: **a**, C1; **b**, C2; **c**, C3; **d**, C4.

richness, and the Shannon index is used to characterize species diversity. The Chao1 and Shannon indexes of group 1F# were obviously lower than those of the other groups. The Chao1 and Shannon indexes of group 0.5F were close to those of 1F and 2F and obviously higher than those of group 4F.

The relative abundances of the sediment bacterial communities at the phylum level are expressed in Fig. 6a. *Firmicutes,* whose relative abundance was 80.0%, was the dominant phylum in the sterilized group. *Proteobacteria*, *Firmicutes*, and *Chloroflexi* were the dominant phyla in the nonsterilized groups, similar to those in the original sediment. The relative abundance of *Proteobacteria* in group 4F was lower than that in groups 0.5F, 1F, and 2F. The relative abundance of *Firmicutes* in group 4F was similar to that in the original sediment and was higher than that in groups 0.5F, 1F, and 2F.

To clarify the differences between bacterial composition within the groups, the relative abundances at the genus level were investigated (Fig. 6b). The main dominant genera in the original sediments were *Thiobacillus* (23.1%), *Paenisporosarcina* (13.8%), *Anaerolineaceae_uncultured* (6.6%), and *SBR1031* (4.4%), which in group 1F# were *Sedimentibacter* (40.4%), *Exiguobacterium* (10.7%), *Anaerovorax* (5.4%), and *Sulfurospirillum* (4.7%). *Thiobacillus*, *Anaerolineaceae_uncultured*, and *SBR1031* were the dominant genera in the other groups. The relative abundances of *Fusibacter* in groups 2F and 4F were higher than those in the other groups. *Trichococcus* (4.8%) was the dominant species in group 4F but was relatively rare in the other groups.

4. Discussion

4.1. The composition and migration of DOM fluorescent components in overlying water and pore water

The spectra of C1 were characterized by excitation peaks at 225 and 275 nm with emission at 345 nm, similar to those of tryptophan-like substances [33]. C2 had a primary fluorescence peak at an Ex/Em wavelength pair of 275/300 nm and a secondary peak at 225/300 nm, representing the presence of protein-like structures similar to tyrosine [34]. C3 (Ex/Em = 235,315/395 nm) resembled microbial humic-like substances, which were linked with relatively aliphatic and low molecular weight compounds [35]. C4 had a primary fluorescence peak at an Ex/Em wavelength pair of 265/450 nm and a secondary peak at 350/450 nm, was assigned to humic-like compounds with relatively high molecular weights [36,37]. C1p (Ex/Em = 225,275/345 nm) was similar to C1 in overlying water and was identified as a tryptophan-like substance. C2p and C3p are tyrosine-like substances [38], similar to C2. C4p was composed of two peaks with excitation maxima at 250 nm and 310 nm at 425 nm emission, which were categorized as a mixture of humic-like and fulvic-like substances [35]. The HIX values of all the samples were lower than 4, which corresponded to weak humification and autochthonous origin [31].

The similarities in DOM fluorescent components between pore water and overlying water indicated the intense exchange of substances at the water-sediment interface. Protein-like substances

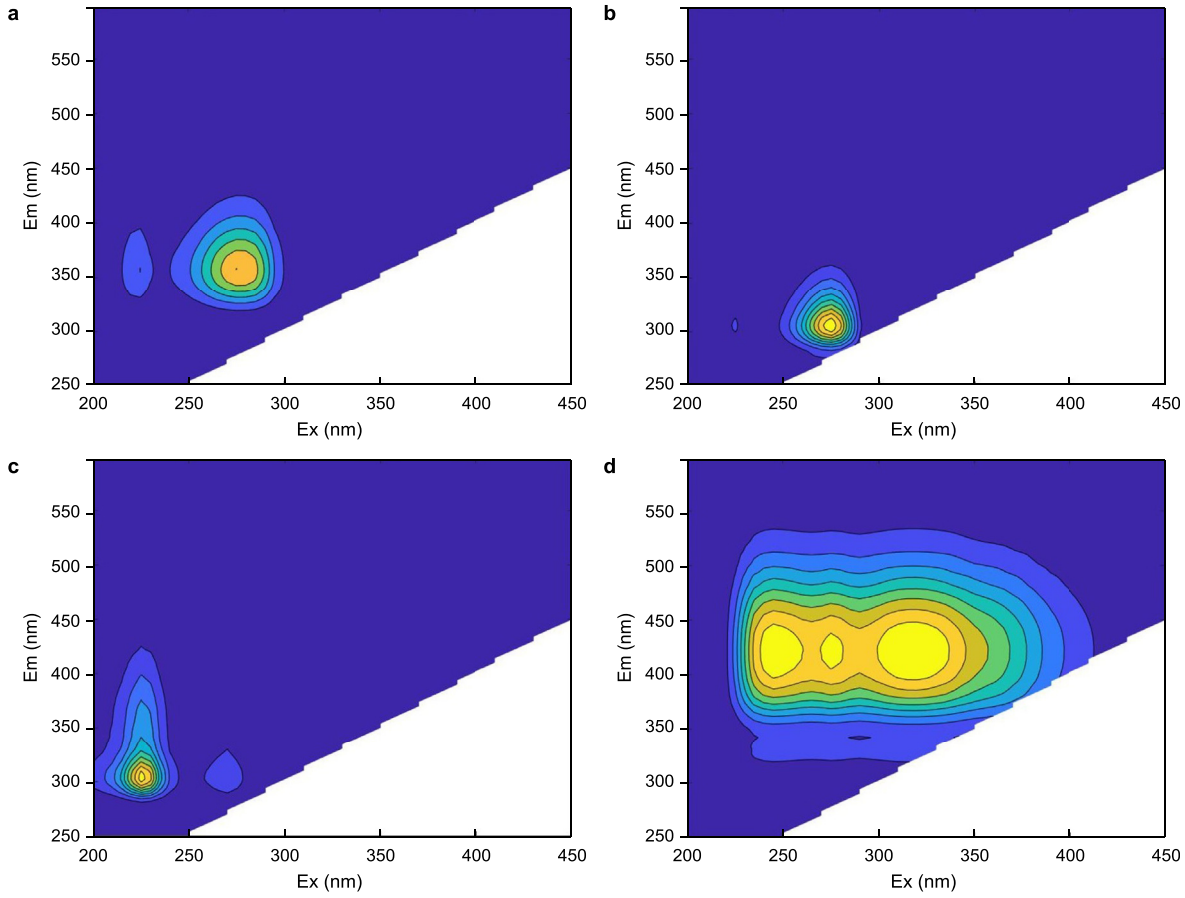

Fig. 5. PARAFAC of DOM in pore water: **a**, C1p; **b**, C2p; **c**, C3p; **d**, C4p.

were the dominant components in both pore water and overlying water. Pore waters have been demonstrated to be a source of protein-like substances to overlying water, and bacteria are the major contributors to protein-like substances via their biological activities, such as metabolism [7,13]. The BIX values of most samples were higher than 1, representing the predominantly autochthonous origin of DOM [39], which emphasized the important role of bacteria on the DOM compositions in both pore water and overlying water. The protein-like fractions in pore water had decreasing trends over time (Fig. A2), which in overlying water had obvious increasing trends in the initial 5 days of the experiment since diffusion resulted in the transport of protein-like fractions from pore water to overlying water. Moreover, protein-like fractions are considered to be preferentially consumed during biodegradation processes [1]. The conversion of humic-like substances into low-molecular-weight substances was reported to be an important process during biodegradation [40,41], which probably occurred in this experiment, as higher HIX values were observed in the sterilized group, suggesting that the degradation of humic-like substances was inhibited when the bacterial activities were decreased. Bacterial degradation is one of the critical reasons for the differences in fluorescent components between overlying water and pore water. Fulvic-like substances in pore water are considered intermediate biodegradation products of humic-like substances [42]. Microbial humic-like substances only existed in overlying water because they were further degraded by bacteria in pore water [43] but were reserved in overlying water due to the lower bacterial activities.

4.2. The influence of pH and F^- on the DOM composition and migration

Pore water was the main source of DOM in the overlying water in this experiment; thus, Pearson's correlation analysis between alpha diversity indexes, environmental factors, and fluorescence characteristics of DOM in pore water at 30 d were conducted to investigate the influencing factors on the DOM composition and migration, and the results are shown in Fig. 7. The pH of pore water showed significant positive correlations with the F_{max} of C1p ($P < 0.01$), C2p ($P < 0.05$), and BIX ($P < 0.05$). The rise in pH contributed to the hydrophilicity and solubilization of DOM because of the deprotonation of weak acid functional groups in the DOM molecules and the increase in the charge density [8,9], which promoted the release of DOM from sediment. The pH of pore water had significant negative correlations with HIX ($P < 0.01$) and a(355) ($P < 0.01$). The increasing release of protein-like components with low molecular weight resulted in a decrease in HIX, accounting for the negative correlations between pH and HIX.

The F^- concentrations did not show significant correlations with the fluorescence characteristics of DOM in pore water. The influence of F^- concentrations was mainly on groups 2F and 4F, which showed the lowest F_{max} of tryptophan-like and tyrosine-like substances in group 2F. Moreover, the lower a(355) in groups 2F and 4F and the proportions of DOM components in group 4F were different from those in other groups in overlying water (Table A3), indicating that F^- concentrations influenced DOM migration. It was speculated that high F^- concentrations indirectly influenced the DOM

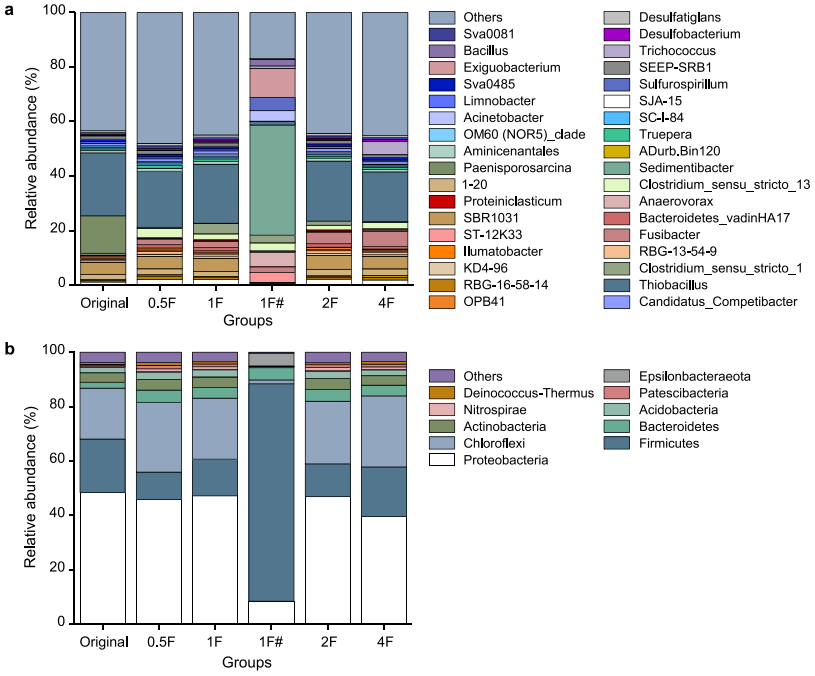

Fig. 6. Bacterial community compositions at the phylum level (**a**) and genus level (**b**) in sediments.

composition and migration via the effect on bacterial activities. F^- was reported to inhibit bacterial abundances in aquatic environments [22], and it usually passes through the cell membrane of bacteria in the form of HF, even under neutral conditions [44]. HF is an effective transmembrane proton conductor [45]; therefore, the toxicity of F^- increases with decreasing pH. As shown in Fig. 2, the pore water was alkaline at first and close to neutral after 5 days; thus, the toxicity of F^- to bacteria increased, resulting in a significant decrease in the F_{max} of C1p, C2p, and C3p after 5 days (Fig. A2). The F_{max} of humic-like substances in group 4F was lower than that in group 1F# but was higher than that in other groups (Fig. A2), suggesting that the influence of high F^- concentrations on DOM composition was similar to that of sterilization, that is, influencing the bacterial communities. Sterilization and high F^- concentrations decreased the bacterial abundances to different extents and then influenced the bacterial-derived products and biodegradation of DOM. As shown in Fig. 7, the Shannon indexes had significant negative correlations with F^- ($P < 0.01$), indicating the repression of F^- on the diversity of bacterial communities. In addition, F^- concentrations caused pH variation in pore water. The HCO_3^- concentrations in pore water increased over time (Fig. A4), indicating that the respiration of bacteria or DOM degradation produced CO_2, which stimulated a decrease in pH. The HCO_3^- concentrations were higher in group 0.5F and lower in groups 2F and 4F, which was consistent with the differences in pH, indicating that high F^- concentrations not only influenced the bacterial abundances (Fig. 7) but also inhibited the respiration of bacteria. Direct or indirect F^- exposure was reported to damage the integrity of the mitochondrial membrane [46], reduce the overall activity of the mitochondria, and inhibit cellular respiration [47]. In addition, the toxicity of F^- probably inhibited the processes of producing acids via some bacteria, such as *Thiobacillus*, which had the highest relative abundances in each group. The SO_4^{2-} concentrations of pore water are shown in Fig. A4. The SO_4^{2-} concentrations had decreasing trends over time because of sediment adsorption and sulfate reduction via *Desulfobacterium*, *Desulfobacca*, etc. The lower pH in group 0.5F promoted the above processes [48,49], resulting in the lowest SO_4^{2-} concentrations. *Thiobacillus* produced H^+ and SO_4^{2-} via sulfur oxidation [50]. The SO_4^{2-} concentrations in group 4F were lower than those in other groups except for group 0.5F, but the pH values in group 4F were maintained at a high level, suggesting that high F^- concentrations inhibited acid production by *Thiobacillus*. Therefore, the negative influence of F^- on bacteria resulted in a significantly lower pH in group 0.5F ($P < 0.05$).

4.3. The response of bacterial community characteristics in sediments to environmental factors and DOM

The richness and relative abundances are described as two key response indicators of bacterial communities to analyze the

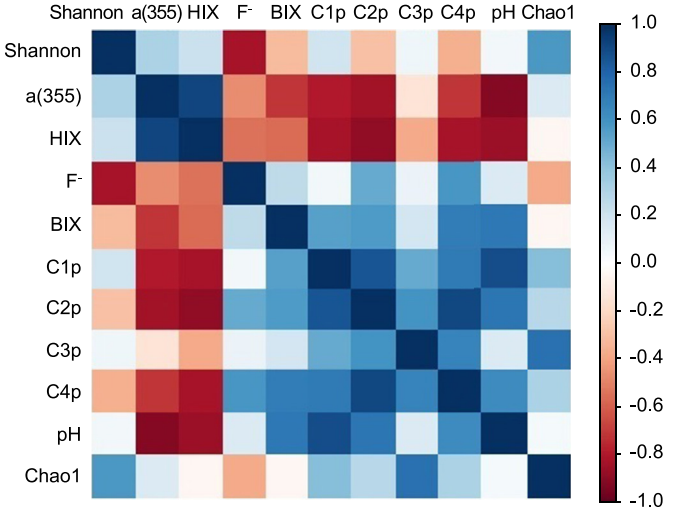

Fig. 7. Pearson's correlations between alpha diversity indexes, environmental factors, and fluorescence characteristics of DOM in pore water.

relationship between sediment bacteria and environmental factors and DOM composition. The Chao1 indexes were significantly positively correlated with the F_{max} of C3p ($P < 0.05$). Previous studies [15,51] have found a positive correlation between bacterial richness and DOM concentrations in both soil and water, revealing that the accumulation of DOM fractions could benefit bacterial abundances, since DOM components provided unique niches for bacterial species to partition.

Among the bacterial phyla, *Proteobacteria* was dominant, and its relative abundance decreased under a 4-fold F^- concentration; this result was consistent with those of previous studies [12,22]. The effect of the F^- concentration on the relative abundance of *Chloroflexi* was small. *Firmicutes* was the most abundant phylum in the sterilized group, and its relative abundance was not inhibited by F^- addition. The relative abundance of *Firmicutes* was reported to be limited by F^- in vitro [52]. *Chloroflexi* and *Firmicutes* were the most abundant phyla in hot water springs with high F^- concentrations [53]. *Chloroflexi* and *Firmicutes* probably have strong resistance to the toxicity of F^-.

To recognize the interaction between the dominant genera relative abundances and DOM components, pH, and F^- concentrations in pore water, redundancy analysis was performed with the data except for that of the sterilized group (Fig. 8). *Thiobacillus* showed positive correlations with the F_{max} of C3p and negative correlations with pH and F^- concentrations. It has been demonstrated that 2 mg L^{-1} F^- can be toxic to *Thiobacillus* and inhibit their growth rates [54]. Few studies have focused on the effect of low F^- concentrations in lake systems on *Thiobacillus*, and the results of this study suggested that lower F^- concentrations in the natural system also had an inhibitory effect on *Thiobacillus* abundances. *Thiobacillus* is an autotrophic sulfur-oxidizing bacterium that decreases the pH during sulfur oxidation [50], which may affect the release of tyrosine-like substances (C3p) indirectly. The genes for tyrosine biosynthesis (EC 2.6.1.57 and 1.3.1.43) are missing in *Thiobacillus ferrooxidans* [55]; however, the extracellular activities of bacteria and cell lysis produce proteins [56], including tyrosine-like components, becoming one of the major reasons for the positive correlation between the F_{max} of C3p and the abundances of *Thiobacillus*, the most dominant species in each group. *Trichococcus* and *Fusibacter* showed positive correlations with F^- concentrations, suggesting their resistance to F^-. *Trichococcus* and *Fusibacter* were positively correlated with the F_{max} of C2p and C4p and negatively correlated with the F_{max} of C1p. *Trichococcus* and *Fusibacter* have the capability of decomposing complex organic matter into simple organic matter [57,58], resulting in the retention of macromolecular humic-like and fulvic-like substances (C4p). *Trichococcus* was proven to be associated with protein degradation under anaerobic conditions [17] and resulted in the accumulation of amino acids. Moreover, *Trichococcus* can metabolize amino acids to produce lactate [59]. In this study, *Trichococcus* probably mainly produced tyrosine-like substances (C2p) via protein degradation and utilized tryptophan-like substances (C1p) to produce lactate. *Fusibacter* showed a similar protein degradation capability to *Trichococcus* [60]; thus, its correlations with the protein-like components were similar to those of *Trichococcus*. *Clostridium_sensu_stricto 13* was positively correlated with the F_{max} of C4p and negatively correlated with the pH and F_{max} of C1p, suggesting that *Clostridium_sensu_stricto 13* participated in the biodegradation of DOM. A previous study found that *Clostridium_sensu_stricto* adapted well to lower pH conditions [61] and was capable of labile DOM utilization and Fe reduction [62], further affecting the composition and migration of DOM. The 4-fold F^- concentration inhibited the alpha diversity indexes of bacteria but promoted the growth of some bacteria associated with DOM transformation, such as *Fusibacter* and *Trichococcus*, which probably accounted for the similarity in the F_{max} values of several DOM components between group 4F and group 1F in the late stages of the experiment.

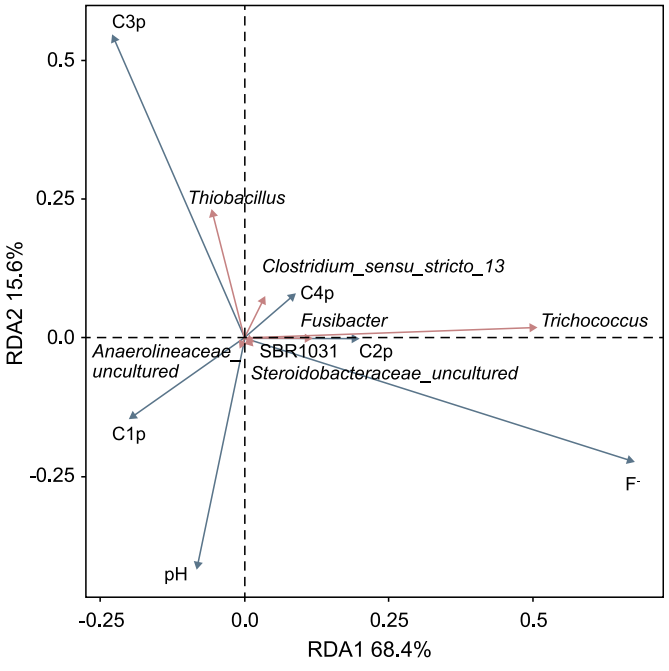

Fig. 8. Redundancy analysis between the dominant genera relative abundances and DOM components, pH, and F^- concentrations in pore water (except for group 1F#); blue arrows represent environmental variables.

4.4. The influence of F^- on the relative abundances of enzymes associated with DOM transformation

The main components of DOM were protein-like substances; thus, the relative abundances of the main enzymes associated with the biosynthesis and metabolism of tryptophan and tyrosine are shown in Fig. 9 and Fig. 10. As shown in Fig. 9, EC:4.1.99.1 (tryptophanase) and EC:4.2.1.20 (tryptophan synthase) mainly participated in the biosynthesis and metabolism of tryptophan. The relative abundances of tryptophanase in groups 2F and 4F were higher than those in groups 0.5F and 1F. Tryptophanase is an enzyme linked to tryptophan degradation. It has been proven that over 85 bacterial species, including the bacteria in Sand Lake sediment such as *Burkholderia* sp., *Clostridium* sp., and *Desulfitobacterium* sp., can produce indole from tryptophan by the catalysis of tryptophanase [63]. The relative abundances of tryptophan synthase in group 4F were higher than those in groups 0.5F and 1F.

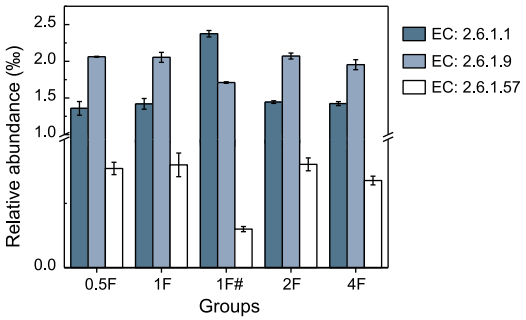

Fig. 9. The relative abundances of the main enzymes associated with the biosynthesis and metabolism of tryptophan.

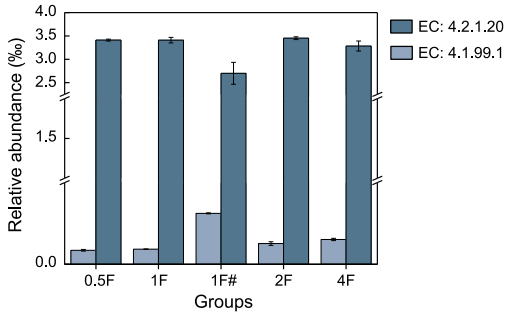

Fig. 10. The relative abundances of the main enzymes associated with the biosynthesis and metabolism of tyrosine.

The results suggested that the high F^- concentrations inhibited the biosynthesis and promoted the degradation of tryptophan-like substances (C1p) by changing the abundances of the relevant enzymes. F^- has long been known to act as an enzyme inhibitor through competition with Mg^{2+} [64], but it can occasionally stimulate enzyme activity, depending on the type of enzyme [65].

As shown in Fig. 10, EC:2.6.1.1 (aspartate transaminase), EC:2.6.1.9 (histidinol-phosphate transaminase), and EC:2.6.1.57 (aromatic-amino-acid transaminase) mainly participated in the biosynthesis and metabolism of tyrosine. Aspartate transaminase and histidinol-phosphate transaminase were associated with the mutual transformation of tyrosine and 4-hydroxyphenylpyruvate. The relative abundance of aspartate transaminase in group 0.5F was lower than that in the other groups. The relative abundance of histidinol-phosphate transaminase in group 4F was lower than that in the other groups except for group 1F#. Aromatic-amino-acid transaminase can catalyze the biosynthesis of tyrosine and the degradation of tyrosine to homogentisate and induce the tyrosine metabolism processes of *Clostridium* sp. [66], one of the dominant bacteria in the Sand Lake sediments. The relative abundance of aromatic-amino-acid transaminase in group 4F was lower than that in the other groups except for group 1F#. It was speculated that the above enzymes primarily acted as catalysts of tyrosine biosynthesis in this study, and the inhibition of aromatic-amino-acid transaminase and histidinol-phosphate by 4-fold F^- concentrations and the decrease in aspartate transaminase caused by 0.5-fold F^- concentrations accounted for the dramatic decrease in tyrosine in groups 0.5 F and 4F over time.

The relative abundances of dominant bacteria and enzymes linked with the transformation of the main DOM components in Sand Lake were influenced by the F^- concentrations; therefore, measures should be taken to limit the increase in F^- concentrations in lake water; otherwise, there is a risk of changing the DOM cycling processes and thus threatening the ecosystem balance, especially in lakes in semiarid regions with fragile aquatic ecosystems.

5. Conclusions

An experiment was performed to ascertain whether and how the fluctuations of F^- concentrations in overlying water affect the composition and migration of DOM from sediment in Sand Lake. The main conclusions are as follows:

(1) Diffusion existed at the water-sediment interface, which resulted in protein-like and humic-like substances in both overlying water and pore water. The higher HIX values in the sterilized group indicated the vital role of bacterial activities in DOM composition. Bacterial activities caused microbial humic-like components in overlying water and fulvic-like components in pore water.

(2) The lowest F^- concentrations in overlying water led to the lowest pH of pore water and overlying water, which was not conducive to DOM release from sediments. Higher F^- concentrations influenced the DOM composition, which caused lower F_{max} values of tryptophan-like and tyrosine-like substances in pore water. The lower a(355) in groups 2F and 4F indicated that F^- concentrations influenced DOM migration.

(3) *Thiobacillus*, *Trichococcus*, and *Fusibacter* were dominant in Sand Lake sediment and played important roles in DOM composition. *Thiobacillus* has the capability to indirectly affect the release of tyrosine-like substances by decreasing pH. *Trichococcus* and *Fusibacter* were positively correlated with the F_{max} of humic-like and fulvic-like components and negatively correlated with the F_{max} of tryptophan-like substances. The increase in F^- concentrations resulted in a decrease in the relative abundance of *Thiobacillus* and an increase in the relative abundance of *Trichococcus* and *Fusibacter*.

(4) High F^- concentrations inhibited biosynthesis and promoted the degradation of tryptophan-like substances. The 4-fold F^- concentrations and 0.5-fold F^- concentrations decreased the abundances of enzymes associated with tyrosine metabolism.

Declaration of interestsDOCI

☒ The authors declare that they have no known competing financial interests or personal relationships that could have appeared to influence the work reported in this paper.

☐The authors declare the following financial interests/personal relationships which may be considered as potential competing interests:

Acknowledgments

This study was supported by the Innovative team project of Nanjing Institute of Environmental Sciences, MEE (GYZX200101), the National Natural Science Foundation of China (No. 51778265), Key R & D Program of Ningxia Hui Autonomous Region (2019BFG02028, 2021BEG01002).

Appendix A. Supplementary data

Supplementary data to this article can be found online at https://doi.org/10.1016/j.ese.2022.100163.

References

[1] C.X. Zhou, Y.D. Liu, C.X. Liu, Y.Y. Liu, M.M. Tfaily, Compositional changes of dissolved organic carbon during its dynamic desorption from hyporheic zone sediments, Sci. Total Environ. 658 (2019) 16–23, https://doi.org/10.1016/j.scitotenv.2018.12.189.

[2] Y.P. Li, S.R. Wang, L. Zhang, H.C. Zhao, L.X. Jiao, Y.L. Zhao, X.S. He, Composition and spectroscopic characteristics of dissolved organic matter extracted from the sediment of Erhai Lake in China, J. Soils Sediments 14 (2014) 1599–1611, https://doi.org/10.1007/s11368-014-0916-2.

[3] Y.W. Wu, Y.J. Li, J.J. Lv, B.D. Xi, L.Y. Zhang, T.X. Yang, G.W. Li, C.L. Li, H.L. Liu, Influence of sediment DOM on environmental factors in shallow eutrophic lakes in the middle reaches of the Yangtze River in China, Environ. Earth Sci. 76 (2017) 142, https://doi.org/10.1007/s12665-017-6427-x.

[4] F. Schmidt, B.P. Koch, T. Goldhammer, M. Elvert, M. Witt, Y.S. Lin, J. Wendt, M. Zabel, V.B. Heuer, K.U. Hinrichs, Unraveling signatures of biogeochemical processes and the depositional setting in the molecular composition of pore water DOM across different marine environments, Geochem. Cosmochim. Acta 207 (2017) 57–80, https://doi.org/10.1016/j.gca.2017.03.005.

[5] M. Derrien, K.H. Shin, J. Hur, Biodegradation-induced signatures in sediment

pore water dissolved organic matter: implications from artificial sediments composed of two contrasting sources, Sci. Total Environ. 694 (2019) 133714, https://doi.org/10.1016/j.scitotenv.2019.133714.
[6] A.N. Loginova, A.W. Dale, F.A.C.L. Moigne, A. Engel, Sediment release of dissolved organic matter to the oxygen minimum zone off Peru, Biogeosciences 17 (2020) 4663–4679, https://doi.org/10.5194/bg-17-4663-2020.
[7] S. Fejjar, A. Melanson, L. Tremblay, Pore waters as a contributor to deep-water amino acids and to deep-water dissolved organic matter concentration and composition in estuarine and marine waters, Mar. Chem. 233 (2021) 103985, https://doi.org/10.1016/j.marchem.2021.103985.
[8] M. Grybos, M. Davranche, G. Gruau, P. Petitjean, M. Pédrot, Increasing pH drives organic matter solubilization from wetland soils under reducing conditions, Geoderma 154 (2009) 13–19, https://doi.org/10.1016/j.geoderma.2009.09.001.
[9] A. Smebye, V. Allinga, R.D. Vogt, T. C Gadmar, J. Mulder, G. Cornelissen, S.E. Hale, Biochar amendment to soil changes dissolved organic matter content and composition, Chemosphere 142 (2016) 100–105, https://doi.org/10.1016/j.chemosphere.2015.04.087.
[10] S.C. Gan, F. Schmidt, V.B. Heuer, T. Goldhammer, M. Witt, K.U. Hinrichs, Impacts of redox conditions on dissolved organic matter (DOM) quality in marine sediments off the River Rhône, Western Mediterranean Sea, Geochem. Cosmochim. Acta 276 (2020) 151–169, https://doi.org/10.1016/j.gca.2020.02.001.
[11] M.L. Chen, J. Hur, Pre-treatments, characteristics, and biogeochemical dynamics of dissolved organic matter in sediments: a review, Water Res. 79 (2015) 10–25, https://doi.org/10.1016/j.watres.2015.04.018.
[12] X.B. Gao, W.T. Luo, X.S. Luo, C.C. Li, X. Zhang, Y.X. Wang, Indigenous microbes induced fluoride release from aquifer sediments, Environ. Pollut. 252 (2019) 580–590, https://doi.org/10.1016/j.envpol.2019.05.118.
[13] X.Q. Wu, L.Y. Wu, Y.N. Liu, P. Zhang, Q.H. Li, J.Z. Zhou, N.J. Hess, T.C. Hazen, W.L. Yang, R. Chakraborty, Microbial interactions with dissolved organic matter drive carbon dynamics and community succession, Front. Microbiol. 9 (2018) 1234, https://doi.org/10.3389/fmicb.2018.01234.
[14] E. Guerrero-Feijóo, M. Nieto-Cid, E. Sintes, V. Dobal-Amador, V. Hernando-Morales, M. Alvarez, V. Balague, M.M. Varela, Optical properties of dissolved organic matter relate to different depth-specific patterns of archaeal and bacterial community structure in the North Atlantic Ocean, FEMS (Fed. Eur. Microbiol. Soc.) Microbiol. Ecol. 93 (2017) fiw224, https://doi.org/10.1093/femsec/fiw224.
[15] M.E. Muscarella, C.M. Boot, C.D. Broeckling, J.T. Lennon, Resource heterogeneity structures aquatic bacterial communities, ISME J. 13 (2019) 2183–2195, https://doi.org/10.1038/s41396-019-0427-7.
[16] P.E. Rossel, C. Bienhold, A. Boetius, T. Dittmar, Dissolved organic matter in pore water of Arctic Ocean sediments: environmental influence on molecular composition, Org. Geochem. 97 (2016) 41–52, https://doi.org/10.1016/j.orggeochem.2016.04.003.
[17] C. Keating, J.P. Chin, D. Hughes, P. Manesiotis, D. Cysneiros, T. Mahony, C.J. Smith, J.W. McGrath, V. O'Flaherty, Biological phosphorus removal during high-rate, low-temperature, anaerobic digestion of wastewater, Front. Microbiol. 7 (2016) 1–14, https://doi.org/10.3389/fmicb.2016.00226.
[18] S. Suominen, N. Dombrowski, J.S.S. Damste, L. Villanueva, A diverse uncultivated microbial community is responsible for organic matter degradation in the Black Sea sulphidic zone, Environ. Microbiol. 23 (2021) 2709–2728, https://doi.org/10.1111/1462-2920.14902.
[19] I. Mukherjee, U.K. Singh, Fluoride abundance and their release mechanisms in groundwater along with associated human health risks in a geologically heterogeneous semi–arid region of east India, Microchem. J. 152 (2020) 104304, https://doi.org/10.1016/j.microc.2019.104304.
[20] V. Ochoa-Herrera, Q. Banihani, G. León, C. Khatri, J.A. Field, R. Sierra-Alvarez, Toxicity of fluoride to microorganisms in biological wastewater treatment systems, Water Res. 43 (2009) 3177–3186, https://doi.org/10.1016/j.watres.2009.04.032.
[21] S.J. Wu, Y. Li, P.H. Wang, L. Zhong, L.Q. Qiu, J.M. Chen, Shifts of microbial community structure in soils of a photovoltaic plant observed using tag-encoded pyrosequencing of 16S rRNA, Appl. Microbiol. Biotechnol. 100 (2016) 3735–3745, https://doi.org/10.1007/s00253-015-7219-4.
[22] X. Zhang, X.B. Gao, C.C. Li, X.S. Luo, Y.X. Wang, Fluoride contributes to the shaping of microbial community in high fluoride groundwater in Qiji County, Yuncheng City, China, Sci. Rep. 9 (2019) 14488, https://doi.org/10.1038/s41598-019-50914-6.
[23] N.R. Johnston, S.A. Strobe, Principles of fluoride toxicity and the cellular response: a review, Arch. Toxicol. 94 (2020) 1051–1069, https://doi.org/10.1007/s00204-020-02687-5.
[24] S. Ali, S.K. Thakur, A. Sarkar, S. Shekhar, Worldwide contamination of water by fluoride, Environ. Chem. Lett. 14 (2019) 291–315, https://doi.org/10.1007/s10311-016-0563-5.
[25] L.F. Tian, X. Zhu, L.M. Wang, F.Q. Peng, Q.Q. Pang, F. He, B. Xu, Distribution, occurrence mechanisms, and management of high fluoride levels in the water, sediment, and soil of Shahu Lake, China, Appl. Geochem. 126 (2021) 104869, https://doi.org/10.1016/j.apgeochem.2021.104869.
[26] L.F. Tian, X. Zhu, L.M. Wang, P. Du, F.Q. Peng, Q.Q. Pang, Long-term trends in water quality and influence of water recharge and climate on the water quality of brackish-water lakes: a case study of Shahu Lake, J. Environ. Manag. 276 (2020) 111290, https://doi.org/10.1016/j.jenvman.2020.111290.
[27] J. Chen, H. Qian, Characterizing replenishment water, lake water and groundwater interactions by numerical modeling in arid region: a case study of Shahu lake, Hydrol. Sci. J. 62 (2017) 104–113, https://doi.org/10.1080/02626667.2015.1133910.
[28] Y.L. Zhang, M.A. Dijk, M.L. Liu, G.W. Zhu, B.Q. Qin, The contribution of phytoplankton degradation to chromophoric dissolved organic matter (CDOM) in eutrophic shallow lakes: field and experimental evidence, Water Res. 43 (2009) 4685–4697, https://doi.org/10.1016/j.watres.2009.07.024.
[29] D.J. Keith, J.A. Yoder, S.A. Freeman, Spatial and temporal distribution of coloured dissolved organic matter (CDOM) in Narragansett Bay, Rhode Island: implications for phytoplankton in coastal waters, Estuarine, Coast. Shelf Sci. 55 (2002) 705–717, https://doi.org/10.1006/ecss.2001.0922.
[30] A. Zsolnay, E. Baigar, M. Jimenez, B. Steinweg, F. Saccomandi, Differentiating with fluorescence spectroscopy the sources of dissolved organic matter in soils subjected to drying, Chemosphere 38 (1999) 45–50, https://doi.org/10.1016/S0045-6535(98)00166-0.
[31] A. Huguet, L. Vacher, S. Relexans, S. Saubusse, E. Parlanti, Properties of fluorescent dissolved organic matter in the Gironde Estuary, Org. Geochem. 40 (2009) 706–719, https://doi.org/10.1016/j.orggeochem.2009.03.002.
[32] A. Zurr, E. Ieno, E. Meesters, A Beginner's Guide to R, Springer, NewYork, 2009, https://doi.org/10.1007/978-0-387-93837-0.
[33] P. Massicotte, J.J. Frenette, Spatial connectivity in a large river system: resolving the sources and fate of dissolved organic matter, Ecol. Appl. 21 (2011) 2600–2617, https://doi.org/10.1890/10-1475.1.
[34] X. Ding, W.H. Xu, Z.W. Li, Phosphate hinders the complexation of dissolved organic matter with copper in lake waters, Environ. Pollut. 276 (2021) 116739, https://doi.org/10.1016/j.envpol.2021.116739.
[35] K.R. Murphy, A. Hambly, S. Singh, R.K. Henderson, S.J. Khan, Organic matter fluorescence in municipal water recycling schemes: toward a unified PARAFAC model, Environ. Sci. Technol. 45 (2011) 2909–2916, https://doi.org/10.1021/es103015e.
[36] K.I. Wheeler, D.F. Levia, J.E. Hudson, Tracking senescence-induced patterns in leaf litter leachate using parallel factor analysis (PARAFAC) modeling and self-organizing maps, J. Geophys. Res. Biogeosci. 122 (2017) 2233–2250, https://doi.org/10.1002/2016JG003677.
[37] X.Y. Zhao, B.D. Xi, W.B. Tan, X. Li, Q.L. Dang, R.F. Li, On the applicability of the 'humic acids' nomenclature from natural ecosystems to engineering sciences, Environ. Sci. Ecotechnol. 6 (2021) 100082, https://doi.org/10.1016/j.ese.2021.100082.
[38] X.T. Xu, J. Kang, J.M. Shen, S.X. Zhao, B.Y. Wang, X.X. Zhang, Z.L. Chen, EEM–PARAFAC characterization of dissolved organic matter and its relationship with disinfection by-products formation potential in drinking water sources of northeastern China, Sci. Total Environ. 774 (2021) 145297, https://doi.org/10.1016/j.scitotenv.2021.145297.
[39] K.M.G. Mostofa, T. Yoshioka, E. Konohira, Dynamics and characteristics of fluorescent dissolved organic matter in the groundwater, river and lake water, Water, Air, and Soil Pollution 184 (2007) 157–176, https://doi.org/10.1007/s11270-007-9405-1.
[40] H.S. Wang, C.P. Feng, Y. Deng, Effect of potassium on nitrate removal from groundwater in agricultural waste-based heterotrophic denitrification system, Sci. Total Environ. 703 (2020) 134830, https://doi.org/10.1016/j.scitotenv.2019.134830.
[41] K.F. Xi, W.F. Hu, D.C. Li, S.F. Jiang, H. Jiang, Investigations on the dissolved organic matter leached from oil-contaminated soils by using pyrolysis remediation method, Sci. Total Environ. 776 (2021) 145921, https://doi.org/10.1016/j.scitotenv.2021.145921.
[42] C.M. Yang, J.L. Sun, Y.Y. Chen, J. Wu, Y.L. Wang, Linkage between water soluble organic matter and bacterial community in sediment from a shallow, eutrophic lake, Lake Chaohu, China, J. Environ. Sci. 98 (2020) 39–46, https://doi.org/10.1016/j.jes.2020.05.023.
[43] J.H. Shi, Y. Zhao, D. Wei, D.Y. Zhang, Z.M. Wei, J.Q. Wu, Insight into transformation of dissolved organic matter in the Heilongjiang River, Environ. Sci. Pollut. Control Ser. 26 (2019) 3340–3349, https://doi.org/10.1007/s11356-018-3761-9.
[44] R.E. Marquis, Antimicrobial actions of fluoride for oral bacteria, Can. J. Microbiol. 41 (1995) 955–964, https://doi.org/10.1139/m95-133.
[45] R.B. Stockbridge, J.L. Robertson, L. Kolmakova-Partensky, C. Miller, A family of fluoride-specific ion channels with dual-topology architecture, Elife 2 (2013), e01084, https://doi.org/10.7554/eLife.01084.
[46] X.Y. Yan, X. Yang, X.H. Hao, Q.R. Ren, J.P. Gao, Y. Wang, N. Chang, Y.L. Qiu, G.H. Song, Sodium fluoride induces apoptosis in H9c2 cardiomyocytes by altering mitochondrial membrane potential and intracellular ROS level, Biol. Trace Elem. Res. 166 (2015) 210–215, https://doi.org/10.1007/s12011-015-0273-z.
[47] B.L. Fina, M. Lombarte, J.P. Rigalli, A. Rigalli, Fluoride increases superoxide production and impairs the respiratory chain in ROS 17/2.8 osteoblastic cells, PLoS One 9 (2014), e100768, https://doi.org/10.1371/journal.pone.0100768.
[48] E. Bayraktarov, R.E. Price, T.G. Ferdelman, K. Finster, The pH and pCO2 dependence of sulfate reduction in shallow-sea hydrothermal CO2–venting sediments (Milos Island, Greece), Front. Microbiol. 4 (2013) 111, https://doi.org/10.3389/fmicb.2013.00111.
[49] L. Martinson, M. Alveteg, The importance of including the pH dependence of sulfate adsorption in a dynamic Soil chemistry model, Water Air Soil Pollut. 154 (2004) 349–356, https://doi.org/10.1023/B:WATE.0000022976.01342.2c.
[50] J.H. Park, S.H. Kim, R.D. Delaune, J.S. Cho, J.S. Heo, Y.S. Ok, D.C. Seo, Enhancement of nitrate removal in constructed wetlands utilizing a combined

autotrophic and heterotrophic denitrification technology for treating hydroponic wastewater containing high nitrate and low organic carbon concentrations, Agric. Water Manag. 162 (2015) 1–14, https://doi.org/10.1016/j.agwat.2015.08.001.
[51] R.T. Bu, T. Ren, M.J. Lei, B. Liu, X.K. Li, R.H. Cong, Y.Y. Zhang, J.W. Lu, Tillage and straw-returning practices effect on soil dissolved organic matter, aggregate fraction and bacteria community under rice-rice-rapeseed rotation system, Agric. Ecosyst. Environ. 287 (2020) 106681, https://doi.org/10.1016/j.agee.2019.106681.
[52] G.J. Chen, P.C. Hua, Z.C. Xu, C.Y. Peng, Y.J. Wang, X.C. Wan, H.M. Cai, The beneficial or detrimental fluoride to gut microbiota depends on its dosages, Ecotoxicol. Environ. Saf. 209 (2021) 111732, https://doi.org/10.1016/j.ecoenv.2020.111732.
[53] M. Tekere, A. Lotter, J. Olivier, N. Jonker, S. Venter, Metagenomic analysis of bacterial diversity of Siloam hot water spring, Limpopo, South Africa, Afr. J. Biotechnol. 10 (2011) 18005–18012, https://doi.org/10.5897/AJB11.899.
[54] M.C. Chen, Y.K. Zhang, B.H. Zhong, L.Y. Qiu, B. Liang, Growth kinetics of *Thiobacilli Strain HSS* and its application in bioleaching phosphate ore, Ind. Eng. Chem. Res. 41 (5) (2002) 1329–1334, https://doi.org/10.1021/ie010064y.
[55] E. Selkov, R. Overbeek, Y. Kogan, L. Chu, V. Vonstein, D. Holmes, S. Silver, R. Haselkorn, M. Fonstein, Functional analysis of gapped microbial genomes: amino acid metabolism of *Thiobacillus ferrooxidans*, Proc. Natl. Acad. Sci. Unit. States Am. 97 (7) (2000) 3509–3514, https://doi.org/10.1073/pnas.97.7.3509.
[56] A.W. Decho, T. Gutierrez, Microbial extracellular polymeric substances (EPSs) in ocean systems, Front. Microbiol. 8 (2017) 922, https://doi.org/10.3389/fmicb.2017.00922.
[57] W.Z. Liu, Z.W. He, C.X. Yang, A.J. Zhou, Z.C. Guo, B. Liang, C. Varrone, A.J. Wang, Microbial network for waste activated sludge cascade utilization in an integrated system of microbial electrolysis and anaerobic fermentation, Biotechnol. Biofuels 9 (2016) 83, https://doi.org/10.1186/s13068-016-0493-2.
[58] R.R. Sun, L. Zhang, Z.F. Zhang, G.H. Chen, F. Jiang, Realizing high-rate sulfur reduction under sulfate-rich conditions in a biological sulfide production system to treat metal-laden wastewater deficient in organic matter, Water Res. 131 (2018) 239–245, https://doi.org/10.1016/j.watres.2017.12.039.
[59] Y.L. Bi, S.Q. Zeng, R. Zhang, Q.Y. Diao, Y. Tu, Effects of dietary energy levels on rumen bacterial community composition in Holstein heifers under the same forage to concentrate ratio condition, BMC Microbiol. 18 (2018) 69, https://doi.org/10.1186/s12866-018-1213-9.
[60] B.R. Song, J.C. Tang, M.N. Zhen, X.M. Liu, Effect of rhamnolipids on enhanced anaerobic degradation of petroleum hydrocarbons in nitrate and sulfate sediments, Sci. Total Environ. 678 (2019) 438–447, https://doi.org/10.1016/j.scitotenv.2019.04.383.
[61] D.Y. Zhao, X.Y. Cao, R. Huang, J. Zeng, Q.L.L. Wu, Variation of bacterial communities in water and sediments during the decomposition of Microcystis biomass, PLoS One 12 (2017), e0176397, https://doi.org/10.1371/journal.pone.0176397.
[62] Y.H. Wang, G.L. Zhang, H.L. Wang, Y. Cheng, H. Liu, Z. Jiang, P. Li, Y.X. Wang, Effects of different dissolved organic matter on microbial communities and arsenic mobilization in aquifers, J. Hazard Mater. 411 (2021) 125146, https://doi.org/10.1016/j.jhazmat.2021.125146.
[63] J.H. Lee, J.T. Lee, Indole as an intercellular signal in microbial communities, FEMS (Fed. Eur. Microbiol. Soc.) Microbiol. Lett. 34 (4) (2010) 426–444, https://doi.org/10.1111/j.1574-6976.2009.00204.x.
[64] A. Strunecka, O. Strunecky, Mechanisms of fluoride toxicity: from enzymes to underlying integrative networks, Appl. Sci. 10 (20) (2020) 7100, https://doi.org/10.3390/app10207100.
[65] O. Barbier, L. Arreola-Mendoza, L.M.D. Razo, Molecular mechanisms of fluoride toxicity, Chem. Biol. Interact. 188 (2) (2010) 319–333, https://doi.org/10.1016/j.cbi.2010.07.011.
[66] D. Dodd, M.H. Spitzer, W. Van Treuren, B.D. Merrill, A.J. Hryckowian, S.K. Higginbottom, A. Le, T.M. Cowan, G.P. Nolan, M.A. Fischbach, J.L. Sonnenburg, A gut bacterial pathway metabolizes aromatic amino acids into nine circulating metabolites, Nature 551 (2017) 648–652, https://doi.org/10.1038/nature24661.